

Dissipation and elliptic flow at RHIC

Dénes Molnár

Department of Physics, Ohio State University, 174 West 18th Ave, Columbus, Ohio 43210, USA

Pasi Huovinen

School of Physics and Astronomy, University of Minnesota, Minneapolis, Minnesota 55455, USA

Helsinki Institute of Physics, P.O. Box 64, FIN-00014 University of Helsinki, Finland and

Department of Physics, P.O. Box 35, FIN-40014 University of Jyväskylä, Finland

(Dated: November 26, 2018)

We compare elliptic flow evolution from ideal hydrodynamics and covariant parton transport theory, and show that, for conditions expected at RHIC, dissipation significantly reduces elliptic flow even for extreme parton cross sections and/or densities $\sigma_{gg} \times dN/d\eta(b=0) \sim 45 \text{ mb} \times 1000$. The difference between transport and hydrodynamic elliptic flow is established rather early during the evolution of the system, but the buildup of elliptic flow is surprisingly insensitive to the choice of the initial (formation or thermalization) time in both models.

PACS numbers: 12.38.Mh, 25.75.-q, 25.75.Ld

Introduction. During the early stage of ultra-relativistic heavy ion collisions at the Relativistic Heavy Ion Collider (RHIC) and the future Large Hadron Collider (LHC), a deconfined phase called the quark-gluon plasma (QGP) is expected to be formed. One way to infer the properties of this dense partonic phase is to study its collective behavior.

An important experimental probe of collective dynamics in noncentral $A + A$ reactions is elliptic flow, $v_2 \equiv \langle \cos(2\phi) \rangle$, the second Fourier moment of the azimuthal momentum distribution [1]. Recent data from RHIC for Au+Au at $\sqrt{s_{NN}} \sim 130 - 200$ GeV show a large anisotropy of particle production in the transverse plane with v_2 values reaching up to 0.2 and saturating in the transverse momentum region $2 < p_{\perp} < 6$ GeV [2, 3].

For $p_{\perp} < 2$ GeV, i.e., for the bulk of the particles produced at RHIC, the elliptic flow data can be reproduced from ideal (Euler) hydrodynamics. In this completely nondissipative theory elliptic flow is sensitive to the equation of state (EOS) of dense nuclear matter [4, 5, 6, 7]. It is remarkable that agreement with the data requires [5, 6, 7] an EOS with deconfinement phase transition, providing one of the strongest arguments for QGP formation at RHIC.

Despite its successes, the assumption of no dissipation has limitations. For example, ideal hydrodynamics fails [8] to saturate elliptic flow for $p_{\perp} > 2$ GeV, and overpredicts [9] the “long” and “out” pion Hanbury-Brown and Twiss (HBT) interferometry radii. Both of these shortcomings are likely due to the neglect of dissipation [10, 11, 12, 13], caused by nonzero mean free paths. In any case, the mere *proof* that the effect of dissipation is negligible (for some observable) already requires a framework that *allows* for dissipation.

For systems near equilibrium, dissipative corrections can be studied via Navier-Stokes (viscous) hydrodynamics. In this theory, the evolution is determined by the

equation of state, the shear and bulk viscosities, and the heat conductivity. Even though a general Lorentz-covariant formulation exists, only 1+1D relativistic solutions are known [14, 15]. Nevertheless, recent estimates [11, 12, 15] find considerable viscous corrections to the evolution of the system, and to spectra, elliptic flow $v_2(p_{\perp})$, and pion HBT parameters at RHIC.

To study dissipative effects arbitrarily far from equilibrium, one can utilize covariant parton transport theory [10, 13, 14, 16, 17, 18, 19]. In this approach elliptic flow depends mainly on the effective scattering cross section of partons produced in the collision [10, 16]. Both the magnitude and the saturation feature of elliptic flow at RHIC can be reproduced [10] if very large (~ 45 mb) elastic parton-parton cross sections are assumed. It is puzzling that these values are an order of magnitude above conventional perturbative QCD (pQCD) estimates. There are, however, recent proposals to alleviate this problem [20, 21].

A popular interpretation of the joint success of ideal hydrodynamics and parton kinetic theory at RHIC is that with ~ 45 mb elastic parton-parton cross sections the opacities are large enough to reach the ideal hydrodynamic limit, at least at $p_T < 2$ GeV. However, that conclusion ignores that calculations based on the two theories corresponded to different initial conditions and thermodynamic properties.

In this paper we provide a systematic comparison of ideal hydrodynamics and transport theory and investigate the importance of dissipative effects at RHIC. Because a thermodynamically consistent microscopic description of the QGP phase transition is still a difficult open problem, we gain insight via studying an ideal gas of massless gluons.

Precursors of this study in Refs. [14, 18] analyzed the transverse energy of particles and found $\sim 20\%$ dissipative corrections. Here we focus on differential elliptic flow

and show that it is more sensitive to dissipation.

Ideal hydrodynamics and covariant transport theory. Ideal (Euler) hydrodynamics is a convenient Lorentz-covariant dynamical theory formulated in terms of macroscopic quantities. In the context of heavy ion collisions, its main advantage is the ability to treat phase transitions, while its main limitation is that it is only applicable to systems in local kinetic equilibrium.

The hydrodynamical equations of motion are the local conservation laws of energy-momentum and net charge

$$\partial_\mu T^{\mu\nu}(x) = 0, \quad \partial_\mu N_c^\mu(x) = 0 \quad (1)$$

[$x \equiv (t, \vec{x})$ is the Minkowski four-coordinate]. In ideal hydrodynamics the energy-momentum tensor is assumed to be that of an ideal fluid, $T^{\mu\nu} = (\epsilon + p)u^\mu u^\nu - pg^{\mu\nu}$, where $\epsilon(x)$, $p(x)$, and $u^\mu(x)$ are the local energy density, pressure, and flow velocity. The charge current is related to the local charge density n_c via $N_c^\mu = n_c u^\mu$. Once the equation of state $p(\epsilon, n_c)$ is specified, Eqs. (1) can be utilized to follow the evolution of the system from any given initial state in local kinetic equilibrium.

For heavy-ion collision applications, hydrodynamics has to be supplemented with a freezeout description because the assumption of local equilibrium breaks down as the local mean free path $\lambda = 1/[\sigma(s)n(x)]$ becomes comparable to the Hubble radius during the expansion. A common approach is to assume that microscopic scattering rates $\Gamma_{sc}(T, n) \sim \sigma(T)n$ drop so quickly that one can consider a *sudden* transition from local equilibrium to a noninteracting gas. In this case, the fluid is converted to particles on a 3D spacetime hypersurface via the Cooper-Frye formula [22]. For systems in chemical equilibrium, a constant temperature (or constant energy density) hypersurface is usually chosen because the only relevant parameter is the temperature, $\Gamma_{sc}(T, n(T))$.

Covariant parton transport theory, in contrast to hydrodynamics, is based on microscopic quantities, namely, the phase space distributions of (quasi)particles and microscopic transition probabilities. The main advantage of this approach is that it is applicable out of equilibrium and models freezeout self-consistently. However, it cannot describe phase transitions (without coupling to classical fields).

We consider here, as in Refs. [10, 13, 14, 16, 17, 18], the simplest but nonlinear form of Lorentz-covariant Boltzmann transport theory in which the on-shell phase space density $f(x, \vec{p})$, evolves with an elastic $2 \rightarrow 2$ rate as

$$p_1^\mu \partial_\mu f_1 = S(x, \vec{p}_1) + \frac{1}{16\pi^2} \iiint_{234} (f_3 f_4 - f_1 f_2) |\overline{\mathcal{M}}_{12 \rightarrow 34}|^2 \times \delta^4(p_1 + p_2 - p_3 - p_4). \quad (2)$$

Here $|\overline{\mathcal{M}}|^2$ is the polarization averaged scattering matrix element squared, the integrals are shorthands for $\int_i \equiv \int d^3 p_i / (2E_i)$, while $f_j \equiv f(x, \vec{p}_j)$. The initial conditions are specified by the source function S . For our

applications below, we interpret $f(x, \vec{p})$ as describing an ultrarelativistic massless gluon gas with $g = 16$ degrees of freedom (8 colors, 2 helicities).

Eq. (2), which corresponds to Boltzmann statistics, could in principle be extended for bosons and/or for inelastic processes, such as $gg \leftrightarrow ggg$. However, no *practical* covariant algorithm yet exists that can handle, at the opacities expected at RHIC, the new nonlinearities these extensions introduce. We therefore limit our study to quadratic dependence of the collision integral on f .

Boltzmann's *H-theorem* states that Eq. (2) drives the system towards a fixed point, global equilibrium. In the *hydrodynamic limit*, i.e., when $|\mathcal{M}|^2 \rightarrow \infty$, the transport evolution approaches the ideal hydrodynamic evolution, $f(x, \vec{p}) = g \exp[(\mu(x) - p_\nu u^\nu(x))/T(x)] / (2\pi)^3$, provided hydrodynamics is *not* frozen out via some prescription. However, for a finite matrix element, an *expanding* system, if it ever equilibrates, sooner or later evolves out of equilibrium (except for very special examples [23]).

Numerical results. We study elliptic flow in a typical midperipheral Au+Au collision at RHIC with impact parameter $b = 8$ fm. The initial conditions were taken from [10]: a longitudinally boost invariant Bjorken tube in local kinetic equilibrium at temperature T_0 at proper time τ_0 fm/c, with a transverse gluon density distribution that is proportional to the binary collision distribution for two Woods-Saxon nuclei. A thermal momentum distribution is necessary because hydrodynamics is limited to such initial conditions. Unlike in usual hydrodynamic calculations, the initial temperature was the same in the entire system even though the density of particles was not. This means that the system was not in chemical equilibrium. Motivated by parton-hadron duality[24], the initial gluon density was normalized to $dN_g/d\eta(b=0) = 1000$ to match the observed $dN_{ch}/d\eta \sim 600$. Accordingly, $dN_g/d\eta \approx 250$ for $b = 8$ fm.

We solved Eq. (2) via the MPC algorithm[25], which utilizes parton subdivision[17, 18] to maintain Lorentz covariance. The elastic parton cross section was isotropic with $\sigma_{tot} = 3, 8,$ and 20 mb, which via transport opacity scaling [10] is approximately equivalent to using a Debye-screened leading-order pQCD $gg \rightarrow gg$ cross section $d\sigma/dt \propto 1/(t - \mu^2)^2$ with $\sigma_{tot} \approx 7, 19,$ and 47 mb. Parton subdivisions of 180 were used to stabilize the numerical results.

The hydrodynamic solutions were obtained via the code used in Refs. [6, 26]. Particle number was conserved explicitly because we are comparing to transport theory with elastic $2 \rightarrow 2$ interactions. For the massless parton gas considered here, the EOS is $\epsilon = 3p$. Because the cross section is energy-independent, freezeout was chosen to occur at a proper density of $n_g = 0.365 \text{ fm}^{-3}$. This corresponds to the gluon density of a chemically equilibrated gluon gas at $T = 120$ MeV.

Figure 1 shows elliptic flow $v_2(p_\perp)$ at freezeout for $T_0 = 700$ MeV and $\tau_0 = 0.1$ fm/c (which are the param-

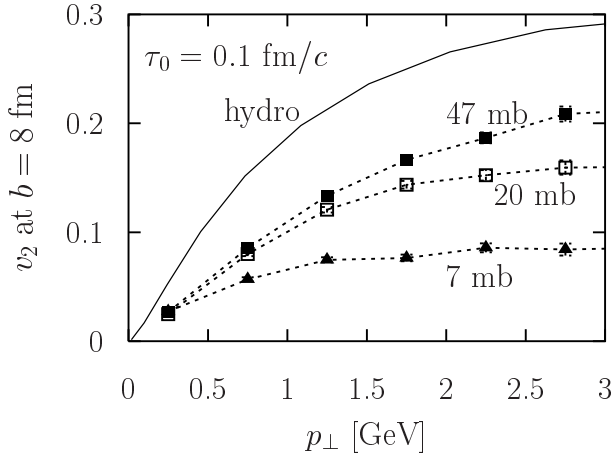


FIG. 1: Comparison of $v_2(p_\perp)$ from ideal hydrodynamics (solid curve) and transport theory as a function of the parton cross section (dashed curves), for $\tau_0 = 0.1$ fm/c.

eters used in [10]). From identical initial conditions and thermodynamic properties ($\epsilon = 3p$ EOS) ideal hydrodynamics produces a much larger anisotropy than transport theory for all three parton cross sections $\sigma_{gg} = 7, 19$, and 47 mb. Even for the largest ~ 45 mb parton cross section studied, dissipation reduces v_2 by 30–40%. This effect is larger by a factor 1.5–2 than what earlier studies [14, 18] found for the final transverse energy dE_T/dy [27].

The reason that both ideal hydrodynamics and parton transport could reproduce the same RHIC v_2 data is that the earlier hydrodynamical calculations utilized a *softer* EOS ($\epsilon > 3p$) that incorporates the QGP phase transition, which reduces elliptic flow. Though dissipative effects for such realistic equations of state are not yet calculable, there is no indication that they would be smaller than for the ideal gas studied here.

The difference between transport and hydrodynamic elliptic flow is established rather early during the evolution, as shown in Fig. 2 where we plot $v_2(p_\perp)$ computed over hypersurfaces of constant τ . Already by $\tau \approx 1$ fm/c, the hydrodynamic anisotropy is a factor two or more above the transport, especially at high p_\perp . The transport v_2 builds up smoothly and at much the same pace both at high and low p_\perp , and by $\tau = 3$ fm/c most ($\sim 80\%$) of the final anisotropy is there. This reinforces the short few-fm/c timescales found for the p_\perp -integrated v_2 in [5, 16]. On the other hand the hydrodynamical development of anisotropy is more p_\perp -dependent. Above $p_\perp = 1$ GeV most (85–90%) of the anisotropy is also developed at $\tau = 3$ fm/c, but at low p_\perp , e.g. at $p_\perp = 0.5$ GeV, anisotropy still increases by a factor of 1.5 before freeze-out at $\tau = 5.3$ fm/c.

A qualitative explanation for the remarkable initial lag in the v_2 evolution for the transport is that for an equilibrium initial condition Eq. (2) in fact corresponds to *free streaming* because the collision term vanishes ex-

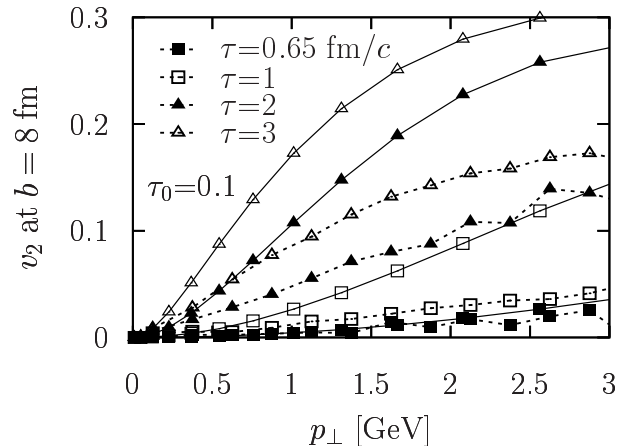


FIG. 2: Time evolution of $v_2(p_\perp)$ from ideal hydrodynamics (solid curves) and transport theory for $\sigma_{gg} = 47$ mb (dashed curves).

actly. Momentum observables can start changing only after the system streams out of equilibrium. In contrast, in hydrodynamics, the initial pressure gradients induce changes in the flow pattern and therefore immediately start to generate elliptic flow.

Because of scalings of the dynamical equations, the above results are quite general. For the transport, the solutions depend only on three scales[10]: T_0 , a trivial scale that fixes the momentum units; and two nontrivial scales $\sigma_{tot}dN/d\eta$ and R/τ_0 . For ideal hydrodynamics, one can similarly prove that three scales apply: T_0 (momentum units), $dN/d\eta$ (linear scale for particle number, e.g., the spectra), and R/τ_0 . For example, for twice larger T_0 and one-third the $dN/d\eta$, the transport $v_2(p_\perp)$ solutions are the same provided σ_{tot} is increased three times and the p_\perp axis is stretched by factor of two, while the hydrodynamic $v_2(p_\perp)$ solutions can be obtained via the stretching of p_\perp axis alone if the freeze-out density is scaled in the same way as the initial density.

Another important difference between the earlier hydrodynamic and transport calculations was that the hydrodynamic evolution started at an assumed *thermalization* time $\tau_0 = 0.6$ fm/c, whereas the transport evolution started at a *formation* time estimate of $\tau_0 = 0.1$ fm/c. One might naively expect that the much smaller initial time for the transport leads to more rapid departure from equilibrium and stronger dissipative effects. However, *for both theories* elliptic flow $v_2(p_\perp)$ is largely insensitive to the initialization time, as shown in Fig. 3 where we compare the above mentioned results for $\tau_0 = 0.1$ fm/c and $T_0 = 700$ MeV with those for $\tau_0 = 0.6$ fm/c and $T_0 = 385$ MeV. To approximately preserve typical particle momenta at freezeout, we have rescaled the initial temperature according to a 1D Bjorken expansion, under which $T \sim \tau^{-1/3}$.

The main reason for the insensitivity to initial time

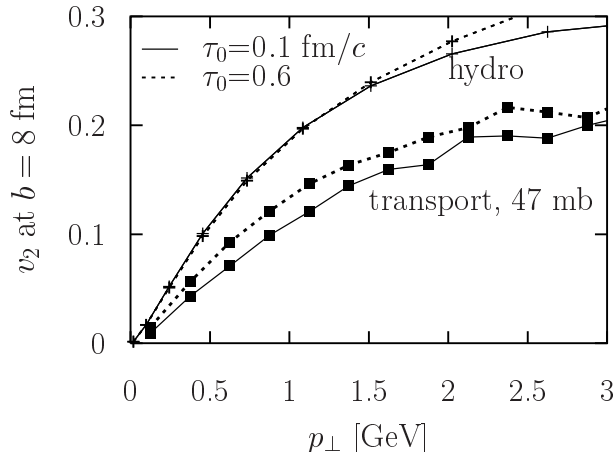


FIG. 3: Weak initialization time dependence of $v_2(p_\perp)$ from ideal hydrodynamics (pluses) and transport theory for $\sigma_{gg} = 47$ mb (boxes).

is that the only relevant parameter that differs between the two calculations, τ_0/R , is in both cases much smaller than one. At early times when $(\tau - \tau_0) \ll R$, the system essentially expands only longitudinally. Therefore, between $\tau = 0.1$ and 0.6 fm/c very little elliptic flow is generated, as can be seen in Fig. 2. Our results reinforce similar findings for ideal hydrodynamics by Ref. [4], and also show that the elliptic flow pattern is largely insensitive to the initial time even in the presence of significant dissipation, as long as $\tau_0 \ll R$.

Conclusions. In this paper we studied elliptic flow $v_2(p_\perp)$ using ideal hydrodynamics and parton transport theory for an ideal gas of massless partons. From identical initial conditions and thermodynamic properties, dissipation significantly reduced $v_2(p_\perp)$, even for extreme ~ 45 mb elastic parton cross sections that are of the order of hadronic cross sections. In addition, comparison to earlier works shows that elliptic flow is more sensitive to dissipation than the final transverse energy.

These results indicate that the large elliptic flow seen at RHIC can be interpreted in (at least) two ways: either as i) a harder nuclear equation of state and strongly dissipative evolution, or ii) a softer equation of state and negligible dissipation which means that the system stays in essentially perfect local kinetic equilibrium via a mechanism whose microscopic origins we do not yet understand.

We emphasize that our results correspond to the simple ideal gas equation of state. A detailed investigation of dissipation in nuclear collisions will have to consider in the future a more realistic nuclear equation of state that includes the hadronization phase transition.

Finally, though our transport solutions do not reach the ideal hydrodynamic limit, it would be very interesting to check how far they are from the Navier-Stokes limit.

Acknowledgments. Helpful discussions with M. Gyulassy and the hospitality of the Columbia University Nuclear Theory Group are gratefully acknowledged. P.H. acknowledges the hospitality of INT Seattle where part of this work was done. This work was supported by DOE grants DE-FG02-01ER41190 and DE-FG02-87ER40328.

lassy and the hospitality of the Columbia University Nuclear Theory Group are gratefully acknowledged. P.H. acknowledges the hospitality of INT Seattle where part of this work was done. This work was supported by DOE grants DE-FG02-01ER41190 and DE-FG02-87ER40328.

-
- [1] For reviews see, e.g., J. Ollitrault, Nucl. Phys. A **638**, 195 (1998); A. M. Poskanzer, nucl-ex/0110013; or S. A. Voloshin, Nucl. Phys. A **715**, 379 (2003).
 - [2] C. Adler *et al.* [STAR Collaboration], Phys. Rev. Lett. **90**, 032301 (2003); K. Filimonov [STAR Collaboration], Nucl. Phys. A **715**, 737 (2003).
 - [3] S. S. Adler *et al.* [PHENIX Collaboration], Phys. Rev. Lett. **91**, 182301 (2003).
 - [4] J. Ollitrault, Phys. Rev. D **46**, 229 (1992).
 - [5] P. F. Kolb, J. Sollfrank and U. Heinz, Phys. Rev. C **62**, 054909 (2000).
 - [6] P. Huovinen *et al.*, Phys. Lett. B **503**, 58 (2001).
 - [7] D. Teaney, J. Lauret and E. V. Shuryak, nucl-th/0110037.
 - [8] R. J. M. Snellings [STAR Collaboration], Nucl. Phys. A **698**, 193 (2002).
 - [9] U. Heinz and P. F. Kolb, Nucl. Phys. A **702**, 269 (2002); D. Zschesche *et al.*, Phys. Rev. C **65**, 064902 (2002).
 - [10] D. Molnar and M. Gyulassy, Nucl. Phys. A **697**, 495 (2002), **A703**, 893(E) (2002); *ibid.* **A698**, 379 (2002).
 - [11] A. Dumitru, nucl-th/0206011.
 - [12] D. Teaney, Nucl. Phys. A **715**, 817 (2003); Phys. Rev. C **68**, 034913 (2003).
 - [13] D. Molnar and M. Gyulassy, Phys. Rev. Lett. **92**, 052301 (2004).
 - [14] M. Gyulassy, Y. Pang and B. Zhang, Nucl. Phys. A **626**, 999 (1997).
 - [15] A. Muronga, nucl-th/0309055; Phys. Rev. Lett. **88**, 062302 (2002) [Erratum-*ibid.* **89**, 159901 (2002)].
 - [16] B. Zhang, M. Gyulassy and C. M. Ko, Phys. Lett. B **455**, 45 (1999).
 - [17] B. Zhang, Comput. Phys. Commun. **109**, 193 (1998).
 - [18] D. Molnar and M. Gyulassy, Phys. Rev. C **62**, 054907 (2000).
 - [19] D. Molnár, Nucl. Phys. A **661**, 236 (1999).
 - [20] D. Molnar and S. A. Voloshin, Phys. Rev. Lett. **91**, 092301 (2003).
 - [21] E. V. Shuryak and I. Zahed, hep-ph/0307267.
 - [22] F. Cooper and G. Frye, Phys. Rev. D **10** (1974) 186.
 - [23] P. Csizmadia, T. Csorgo and B. Lukacs, Phys. Lett. B **443**, 21 (1998).
 - [24] K. J. Eskola, K. Kajantie, P. V. Ruuskanen, and K. Tuominen, Nucl. Phys. B **570**, 379 (2000) [hep-ph/9909456].
 - [25] D. Molnár, MPC 1.6.0. This parton cascade code used in the present study can be downloaded from WWW at <http://nt3.phys.columbia.edu/people/molnard>.
 - [26] P. F. Kolb *et al.*, Phys. Lett. B **500**, 232 (2001); Nucl. Phys. A **696**, 197 (2001).
 - [27] See, e.g., Fig. 1 in [18]. The open squares there correspond to the $\sigma_{gg} = 47$ mb case in this study.